

Spin pumping by a moving domain wall at the interface of an antiferromagnetic insulator and a two-dimensional metal

A. G. Mal'shukov

Institute of Spectroscopy, Russian Academy of Sciences, Troitsk, Moscow, 108840, Russia

A domain wall (DW) which moves parallel to a magnetically compensated interface between an antiferromagnetic insulator (AFMI) and a two-dimensional (2D) metal can pump spin polarization into the metal. It is assumed that localized spins of a collinear AFMI interact with itinerant electrons through their exchange interaction on the interface. We employed the formalism of Keldysh Green's functions for electrons which experience potential and spin-orbit scattering on random impurities. This formalism allows a unified analysis of spin pumping, spin diffusion and spin relaxation effects on a 2D electron gas. It is shown that the pumping of a nonstaggered magnetization into the metal film takes place in the second order with respect to the interface exchange interaction. At sufficiently weak spin relaxation this pumping effect can be much stronger than the first-order effect of the Pauli magnetism which is produced by the small nonstaggered exchange field of the DW. It is shown that the pumped polarization is sensitive to the geometry of the electron's Fermi surface and increases when the wave vector of the staggered magnetization approaches the nesting vector of the Fermi surface. In a disordered diffusive electron gas the induced spin polarization follows the motion of the domain wall. It is distributed asymmetrically around the DW over a distance which can be much larger than the DW width.

I. INTRODUCTION

Antiferromagnets (AFM) have drawn growing interest recently due to their potential use for various spintronic applications. One of the most important characteristics of spintronic devices is their ability to transmit and control spin polarization. From this point of view AFM materials demonstrate numerous interesting features. The progress made in this field was presented in several reviews (see, for instance¹⁻⁴). Considerable progress has been achieved in understanding of mechanisms for angular moment transfer between spins of localized and itinerant electrons in metallic AFM, as well as interface spin transfer between a normal metal and a metallic or insulating AFM⁵⁻¹¹. These mechanisms allow to control localized spins of AFM, as well as spins of itinerant electrons. For instance, the spin current of electrons produces the torque effect on the staggered AFM magnetization. Recent experimental studies have demonstrated that this torque results in rotation of the magnetization and its switching^{4,12-14}. Alternatively, when the Néel order varies in time the magnetization can be pumped through the interface into the electron gas of a paramagnetic metal which makes a contact with an AFM^{6,15}. In this case the spin polarization may be delivered to the interface by spin waves^{6,16-18}, or by moving topological defects, like DWs and skyrmions. Compared with ferromagnets, spin waves and topological spin textures exhibit much faster dynamics in AFMs. For instance, in antiferromagnetic insulators spin waves can propagate over relatively large (submicron) distances²⁰ and DWs can move much faster than in ferromagnets^{21,22}. These outstanding features of conducting and insulating antiferromagnets form the basis for their future applications in spintronic devices.

So far, the activity in studying the spin pumping from an AFMI into a normal metal was focused on three di-

mensional (3D) metals. On the other hand, there is a great interest in heterostructures which are combined of magnetic systems and 2D metals. In particular, this interest is caused by recent success in creating of various 2D van der Waals metallic and insulating systems. However, the problem of spin pumping from an AFMI's space-time dependent spin texture into a 2D metal film was not addressed in literature. At the same time, there are some significant distinctions between 3D and 2D cases. First of all, 2D electrons undergo scattering from an interfacial spin texture which has the same 2D dimensionality. Therefore, constructive interference of spin dependent scattering amplitudes from two AFM sublattices can result in a strong enhancement of the scattering probability. This effect becomes important when the Fermi surface reveals nesting parts with roughly the same wave vector as that of the staggered magnetization. In contrast, in 3D systems such an interference effect is smeared out due to integration over k_z , where k_z is the component of the electron's wave-vector which is perpendicular to the interface. One more specific feature of 2D systems is that electronic transport takes place along the interface, so that electrons are always in contact with localized spins of the AFM, while in 3D systems the angular momentum, which electrons obtain from a dynamic AFMI texture, is carried away from the interface. Therefore, with a good accuracy a 3D metal can be considered as a spin sink for electrons, that is not true for 2D systems. In the former case, the angular moment transfer is controlled by the so called interface spin mixing conductance^{6,19} which is simply a local characteristic of a given interface. Such an approach can not be applied for the analysis of the spin transfer across the AFMI/2D metal interface, because it is closely related to the lateral transport of 2D electrons. Therefore, one needs a unified theory which combines quantum dynamics of 2D electrons with their scattering from a space-time dependent spin texture of

AFMI.

In this context the problem of spin pumping by a domain wall, which moves along the magnetically compensated interface, has not been addressed so far. To solve this problem we employ the Keldysh²³ formalism of nonequilibrium Green's functions for a disordered 2D electron gas which interacts with localized spins of an adjacent AFMI by means of the exchange interaction J . Besides the potential scattering from random impurities, the spin-orbit scattering of electrons will also be taken into account. The latter gives rise to relaxation of the spin polarization of itinerant electrons. As a result, in the diffusive regime the spin density distribution will diffusively evolve in space and decrease in time with some spin relaxation rate.

This problem will be considered within a simple tight binding model where 2D and AFMI lattices form a commensurate contact. The exchange interaction is treated within the perturbation theory which is valid when $J \ll E_F$, where E_F is the Fermi energy of conduction electrons. The Fermi level is placed not too close to the van Hove singularity, where a gap in the electron band energy is formed due to the interface exchange interaction with AFMI.¹ Within the perturbation theory the pumping of (nonstaggered) spin polarization into a normal metal by the staggered Néel magnetization takes place only in even orders of the perturbational expansion with respect to J . On the other hand, besides the staggered magnetization, a time dependent spin texture of a moving DW carries a small nonstaggered component²⁴ which is localized near the DW. In turn, due to the interface exchange interaction such a "ferromagnetic" magnetization polarizes spins of itinerant electrons in adjacent normal metal already in the first order by J . However, as it will be shown, in a reasonable range of parameters the effect of second order perturbational terms may exceed considerably that of the first order ones, because these competing effects involve very different physical mechanisms. Indeed, in the former case the angular momentum, which is carried by a DW, is transferred through the interface to electrons. This process leads to accumulation of the electron's spin polarization near DW and, as it will be shown, the latter increases with the spin relaxation time. In contrast, the first-order effect is simply the Pauli magnetization. In the absence of spin relaxation it does not increase in time. Instead, it simply redistributes in space, by following the motion of the DW.

The article is organized in the following way. In Sec. II a general formalism of the spin density response in a 2D disordered electron gas to a moving DW is expressed in terms of Green's functions, up to the second-order with respect to the exchange interaction. Sec. III is devoted to calculations of the spin polarization. The results are discussed in Sec. IV. Two sections are added in the Appendix in order to clarify some details of calculations.

II. GENERAL FORMALISM

A. Basic equations

In this section we express the spin polarization in 2D electron gas as an expansion over the exchange interaction between itinerant electrons and localized spins of an adjacent AFMI. By assuming that the 2D lattice of the normal metal is commensurate with the lattice of localized spins on the AFMI interface and that metal atoms make an on-top contact with atoms of the AFMI, the exchange interaction can be written in the form

$$M = J \sum_i c_i^+ \mathbf{S}_i(t) \cdot \boldsymbol{\sigma} c_i. \quad (1)$$

where $c_i^+ = (c_{i\uparrow}^+, c_{i\downarrow}^+)$ is the two-component creation operator of an electron whose spin projections are \uparrow , or \downarrow and c_i is the conjugate to c_i^+ destruction operator. The vector $\mathbf{S}_i(t)$ represents a spin which is localized on the lattice site \mathbf{r}_i and $\boldsymbol{\sigma} = (\sigma_x, \sigma_y, \sigma_z)$ is the vector of Pauli matrices. Since there are two sublattices, the lattice sites will be denoted as $i1$ and $i2$. Correspondingly, spins localized on these sublattices will be denoted as \mathbf{S}_{i1} and \mathbf{S}_{i2} . These spins are treated as classical variables satisfying the constraint $|\mathbf{S}_i(t)| = S$. In many practical situations \mathbf{S}_i varies slowly within each of two AFM sublattices. Therefore, one may introduce two vector fields $\mathbf{m}_1(\mathbf{r}, t)$ and $\mathbf{m}_2(\mathbf{r}, t)$, which are defined on sublattices 1 and 2, respectively, where $\mathbf{m}_{1(2)}(\mathbf{r}_i, t) = \mathbf{S}_{i1(2)}/S$. The Néel order is given by the unit vector field $\mathbf{n}(\mathbf{r}, t) = (\mathbf{m}_1(\mathbf{r}, t) - \mathbf{m}_2(\mathbf{r}, t))/|\mathbf{m}_1(\mathbf{r}, t) - \mathbf{m}_2(\mathbf{r}, t)|$. Due to the strong exchange coupling of spins in different sublattices we have $\mathbf{m}_1(\mathbf{r}, t) \simeq -\mathbf{m}_2(\mathbf{r}, t)$. Therefore, the nonstaggered field $\mathbf{m}(\mathbf{r}, t) = (\mathbf{m}_1(\mathbf{r}, t) + \mathbf{m}_2(\mathbf{r}, t))/2 \ll 1$. In this case by using the Landau-Lifshitz-Gilbert equation \mathbf{m} can be expressed²⁴ in terms of \mathbf{n} , as

$$\mathbf{m}(\mathbf{r}, t) = \frac{1}{E_{\text{ex}}} (\partial_t \mathbf{n}(\mathbf{r}, t) \times \mathbf{n}(\mathbf{r}, t)), \quad (2)$$

where E_{ex} is the exchange energy of near-neighbor spins in AFM. Further, by expressing the operators c_i as $c_i = \sum_{\mathbf{k}} c_{\mathbf{k}} \exp i\mathbf{k}\mathbf{r}_i$, matrix elements of the exchange interaction in Eq.(1) can be written in terms of $\mathbf{n}_{\mathbf{f}}(t)$ and $\mathbf{m}_{\mathbf{f}}(t)$, which are spatial Fourier transforms of these fields with the wave vector \mathbf{f} . These matrix elements are given by

$$M_{\mathbf{k}+\mathbf{f}, \mathbf{k}}(t) = JS [c_{\mathbf{k}+\mathbf{f}+\mathbf{G}}^+ \mathbf{n}_{\mathbf{f}}(t) \boldsymbol{\sigma} c_{\mathbf{k}} + c_{\mathbf{k}+\mathbf{f}}^+ \mathbf{m}_{\mathbf{f}}(t) \boldsymbol{\sigma} c_{\mathbf{k}}], \quad (3)$$

where $\mathbf{G} = (G_x, G_y)$ is the umklapp vector which is associated with the AFM's staggered magnetization, so that for the square lattice $G_x = \pm\pi/a$ and $G_y = \pm\pi/a$. In contrast, the vector \mathbf{f} is small, namely, $f \ll 1/a$, where a is the lattice constant. It is because relatively slow spatial variations of $\mathbf{n}(\mathbf{r}, t)$ and $\mathbf{m}(\mathbf{r}, t)$ are determined by the spin texture of DW whose width is assumed to be much larger than a .

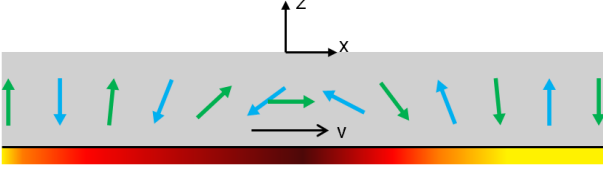


FIG. 1: (Color online) A bilayer system is composed of an antiferromagnetic insulator and a 2D paramagnetic metal film. A domain wall which moves from left to right with the velocity v leads to spin accumulation in the metal film. The spin is oriented parallel to the y -axis. The corresponding spin density (shown by color) is asymmetrically distributed around DW over distances which can be much larger than the width of the DW.

The induced spin density of electrons can be expressed in terms of the Keldysh^{23,25} function $G^K(\mathbf{r}, t; \mathbf{r}', t')$, which is a 2×2 matrix in the spin space. This expression has the form

$$\mathbf{S}(\mathbf{r}, t) = -\frac{i}{4} \text{Tr}[\boldsymbol{\sigma} \langle G^K(\mathbf{r}, t; \mathbf{r}, t) \rangle_{\text{imp}}], \quad (4)$$

where $\langle \dots \rangle_{\text{imp}}$ denotes averaging over impurity positions. The Keldysh function, in turn, is given by the perturbational expansion over the exchange interaction M . The corresponding correction $\delta G^K(\mathbf{q}, \omega)$ to the space-time Fourier transform of $G^K(\mathbf{r}, t; \mathbf{r}, t)$ can be written in terms of the unperturbed Green's functions $G_{\mathbf{k}, \mathbf{k}'}^K(\omega)$, $G_{\mathbf{k}, \mathbf{k}'}^r(\omega)$ and $G_{\mathbf{k}, \mathbf{k}'}^a(\omega)$, which are, respectively, the Keldysh, retarded and advanced ones. These functions are not averaged over impurity positions. Therefore, they depend on the two wave vectors \mathbf{k} and \mathbf{k}' . They may be represented by the 2×2 matrix $\hat{G}_{\mathbf{k}, \mathbf{k}'}(\omega)$ which is given by

$$\hat{G}_{\mathbf{k}, \mathbf{k}'}(\omega) = \begin{bmatrix} G_{\mathbf{k}, \mathbf{k}'}^r(\omega) & G_{\mathbf{k}, \mathbf{k}'}^K(\omega) \\ 0 & G_{\mathbf{k}, \mathbf{k}'}^a(\omega) \end{bmatrix}, \quad (5)$$

where in thermal equilibrium $G_{\mathbf{k}, \mathbf{k}'}^K(\omega)$ has the form

$$G_{\mathbf{k}, \mathbf{k}'}^K(\omega) = (G_{\mathbf{k}, \mathbf{k}'}^r(\omega) - G_{\mathbf{k}, \mathbf{k}'}^a(\omega)) \tanh(\omega/2k_B T) \quad (6)$$

Within the Keldysh formalism^{23,25} the correction $\delta G^K(\mathbf{q}, \omega)$ is given by

$$\delta G^K(\mathbf{q}, \omega) = \int \frac{d\omega'}{2\pi} \sum_{\mathbf{k}, \mathbf{p}, \mathbf{p}'} \left[\hat{G}_{\mathbf{k}^+, \mathbf{p}^+}(\omega'^+) \times \hat{\Sigma}_{\mathbf{p}, \mathbf{p}'}(\omega', \omega, \mathbf{q}) \hat{G}_{\mathbf{p}'^-, \mathbf{k}^-}(\omega'^-) \right]^K, \quad (7)$$

where $\omega'^{\pm} = \omega' \pm \omega/2$, $\mathbf{k}^{\pm} = \mathbf{k} \pm \mathbf{q}/2$ and the superscript "K" denotes the Keldysh component of the matrix product in Eq.(7). By performing the time Fourier transform of $\mathbf{n}_{\mathbf{f}}(t)$ and $\mathbf{m}_{\mathbf{f}}(t)$ in Eq.(3) one can express $\hat{\Sigma}$ in the form

$$\hat{\Sigma}_{\mathbf{p}, \mathbf{p}'}(\omega', \omega, \mathbf{q}) = \hat{\Sigma}^{(1)}(\omega, \mathbf{q}) \delta_{\mathbf{p}, \mathbf{p}'} + \int \frac{d\nu}{2\pi} \sum_{\mathbf{f}} \hat{\Sigma}_{\mathbf{p}, \mathbf{p}'}^{(2)}(\omega', \omega, \mathbf{q}; \nu, \mathbf{f}), \quad (8)$$

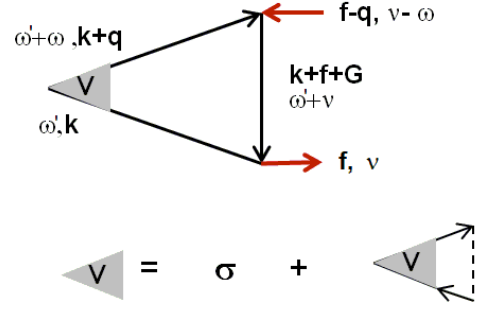


FIG. 2: (Color online) a) A second-order Feynman diagram for the spin density $\mathbf{S}(\mathbf{q}, \omega)$, which is induced by a moving domain wall. The DW perturbation Eq.(3) is shown by red arrows. b) The Bethe-Salpeter equation for the spin diffusion vertex \mathbf{V} , where $\boldsymbol{\sigma}$ is the vector of Pauli matrices. Elastic scattering from random impurities is shown by the dashed line.

where the functions $\hat{\Sigma}^{(1)}$ and $\hat{\Sigma}^{(2)}$ correspond to the first-order and second-order corrections, respectively. They are given by

$$\hat{\Sigma}^{(1)}(\omega, \mathbf{q}) = \hat{1} J S \boldsymbol{\sigma} \mathbf{m}_{\mathbf{q}, \omega} \quad (9)$$

and

$$\hat{\Sigma}_{\mathbf{p}, \mathbf{p}'}^{(2)}(\omega', \omega, \mathbf{q}; \nu, \mathbf{f}) = 2J^2 S^2 (\boldsymbol{\sigma} \mathbf{n}_{\mathbf{f}^+, \nu^+}) \times \hat{G}_{\mathbf{p}-\mathbf{f}+\mathbf{G}, \mathbf{p}'-\mathbf{f}+\mathbf{G}}(\omega' - \nu) (\boldsymbol{\sigma} \mathbf{n}_{\mathbf{f}^-, \nu^-}), \quad (10)$$

where $\nu^{\pm} = \nu \pm \omega/2$, $\mathbf{f}^{\pm} = \mathbf{f} \pm \mathbf{q}/2$ and $\hat{1}$ is the unit matrix in the Keldysh space.

The second order contribution to $\mathbf{S}(\mathbf{r}, t)$ is shown as a Feynman diagram in Fig.2, while the first-order term is given by a usual fermion loop. The averaging in Eq.(4) over random positions of impurities results²⁶ in the occurrence of average Green functions and the vertex \mathbf{V} in Fig.2. This vertex describes multiple scattering processes which result in diffusion of particles and their spin relaxation. Within the Born approximation the calculation of \mathbf{V} is reduced to a solving of the Bethe-Salpeter equation which is graphically shown in Fig.2. The multiple scattering processes are important when the frequency and momentum transfer in the vertex are much smaller than $\Gamma = 1/2\tau$ and $1/l$, where τ and l are the elastic scattering time and electron mean free path, respectively. Therefore, from Fig.2 it is seen that such a diffusion regime takes place when $\omega \ll \Gamma$ and $q \ll 1/l$. At the same time, the vertices which are associated with the exchange interaction of electrons with the staggered magnetization retain unrenormalized, because of the large momentum transfer $\sim \mathbf{G}$ caused by such a magnetization. By using Eqs.(5,6) and Eqs.(9,10) one may express $\langle \delta G^K \rangle_{\text{imp}}$ in Eq.(7), as well as the space-time Fourier transform $\mathbf{S}(\mathbf{q}, \omega)$ of Eq.(4), in terms of averaged retarded and advanced Green's functions. The total spin polarization may be represented by a sum of terms which are renormalized by \mathbf{V} and those which are not. The former will

be denoted as $\mathbf{S}_V(\mathbf{q}, \omega)$. It includes only vertices which involve the product of retarded and advanced functions in the ladder series. Otherwise, the renormalization is not important²⁶. At the same time the unrenormalized term is given by the bare vertex $\boldsymbol{\sigma}$ instead of \mathbf{V} . The corresponding bare contribution to $\mathbf{S}(\mathbf{q}, \omega)$ will be denoted as $\mathbf{S}_0(\mathbf{q}, \omega)$.

It is convenient to express the products of Green's functions in Eq.(7) in terms of retarded and advanced functions by using Eqs.(5) and (6). For example, the "Keldysh" component (12 matrix component in Eq.(5)) of a product of three functions can be written as

$$\begin{aligned} (G_1 G_2 G_3)^K &= (G_1^r - G_1^a) G_2^a G_3^a \tanh \frac{\omega_1}{2k_B T} + \\ &G_1^r (G_2^r - G_2^a) G_3^a \tanh \frac{\omega_2}{2k_B T} + \\ &G_1^r G_2^r (G_3^r - G_3^a) \tanh \frac{\omega_3}{2k_B T}, \end{aligned} \quad (11)$$

where the subscripts 1,2,3 denote variables of the Green functions. By combining all terms, which are generated by the product of Keldysh matrices in Eq.(7), we arrive at $\mathbf{S} = \mathbf{S}_V^{(1)} + \mathbf{S}_V^{(2)} + \mathbf{S}_0^{(1)} + \mathbf{S}_0^{(2)}$, where

$$\begin{aligned} \mathbf{S}_V^{(1)}(\mathbf{q}, \omega) &= -\frac{i}{4} \sum_{\mathbf{k}} \int \frac{d\omega'}{2\pi} \text{Tr}[\mathbf{V}(\omega, \mathbf{q}) G_{\mathbf{k}^+}^r(\omega'^+) \times \\ &\Sigma^{(1)}(\omega, \mathbf{q}) G_{\mathbf{k}^-}^a(\omega'^-)] \left(\tanh \frac{\omega'^+}{2k_B T} - \tanh \frac{\omega'^-}{2k_B T} \right), \end{aligned} \quad (12)$$

$$\begin{aligned} \mathbf{S}_0^{(1)}(\mathbf{q}, \omega) &= -\frac{i}{4} \sum_{\mathbf{k}} \int \frac{d\omega'}{2\pi} \text{Tr} \left[\boldsymbol{\sigma} G_{\mathbf{k}^+}^r(\omega'^+) \Sigma^{(1)}(\omega, \mathbf{q}) \times \right. \\ &G_{\mathbf{k}^-}^r(\omega'^-) \tanh \frac{\omega'^-}{2k_B T} - \boldsymbol{\sigma} G_{\mathbf{k}^+}^a(\omega'^+) \Sigma^{(1)}(\omega, \mathbf{q}) \times \\ &\left. G_{\mathbf{k}^-}^a(\omega'^-) \tanh \frac{\omega'^+}{2k_B T} \right], \end{aligned} \quad (13)$$

$$\begin{aligned} \mathbf{S}_V^{(2)}(\mathbf{q}, \omega) &= -\frac{i}{4} \sum_{\mathbf{k}, \mathbf{f}} \int \frac{d\omega'}{2\pi} \frac{d\nu}{2\pi} \text{Tr} \left[\mathbf{V}(\omega, \mathbf{q}) (P^{raa}(\omega'^+) \right. \\ &\left. - P^{rra}(\omega'^-) + P^{rra}(\omega' - \nu) - P^{raa}(\omega' - \nu)) \right] \end{aligned} \quad (14)$$

and

$$\begin{aligned} \mathbf{S}_0^{(2)}(\mathbf{q}, \omega) &= -\frac{i}{4} \sum_{\mathbf{k}, \mathbf{f}} \int \frac{d\omega'}{2\pi} \frac{d\nu}{2\pi} \text{Tr} \left[\boldsymbol{\sigma} (P^{rrr}(\omega'^-) - \right. \\ &\left. P^{aaa}(\omega'^+)) \right], \end{aligned} \quad (15)$$

where the functions $P^{ijk}(\Omega)$, with $\Omega = \omega'^{\pm}$ and $\Omega = \omega' - \nu$, are given by

$$\begin{aligned} P^{ijk}(\Omega) &= G_{\mathbf{k}^+}^i(\omega'^+) \Sigma_{\mathbf{k}}^{(2)j}(\omega', \omega, \mathbf{q}; \nu, \mathbf{f}) \times \\ &G_{\mathbf{k}^-}^k(\omega'^-) \tanh \left(\frac{\Omega}{2k_B T} \right), \end{aligned} \quad (16)$$

where $G_{\mathbf{k}}^i(\omega) = \langle G_{\mathbf{k}, \mathbf{k}'}^i(\omega) \rangle_{\text{imp}} \delta_{\mathbf{k}, \mathbf{k}'}$, $\Sigma_{\mathbf{k}}^{(2)i}(\omega', \omega, \mathbf{q}; \nu, f) = \langle \Sigma_{\mathbf{k}, \mathbf{k}'}^{(2)i}(\omega', \omega, \mathbf{q}; \nu, f) \rangle_{\text{imp}} \delta_{\mathbf{k}, \mathbf{k}'}$ and $i = r, a$. It follows from Eq.(10) that after the averaging over impurity positions the function $\Sigma_{\mathbf{k}, \mathbf{k}'}^{(2)i}(\omega', \omega, \mathbf{q}; \nu, f)$ becomes

$$\begin{aligned} \Sigma_{\mathbf{k}}^{(2)i}(\omega', \omega, \mathbf{q}; \nu, f) &= 2J^2 S^2 (\boldsymbol{\sigma} \mathbf{n}_{\mathbf{f}^+, \nu^+}) \times \\ &G_{\mathbf{k}-\mathbf{f}+\mathbf{G}}^i(\omega' - \nu) (\boldsymbol{\sigma} \mathbf{n}_{\mathbf{f}^-, \nu^-}). \end{aligned} \quad (17)$$

Eqs.(12)-(17) form a basis for calculation of the spin density created by DW in 2D gas. The sum of the terms, that are given by Eqs.(12) and (13), represents the spin density induced by the interaction $J S \boldsymbol{\sigma} \mathbf{m}_{\mathbf{q}, \omega}$ of electron spins with the nonstaggered Zeeman field $J S \mathbf{m}_{\mathbf{q}, \omega}$. It is expressed in terms of the space-time dependent Pauli susceptibility, which is given by a single fermion loop, where the multiple scattering from impurities is taken into account in a standard way through the vertex function \mathbf{V} .^{25,26} At the same time, Eqs.(14) and (15) represent the effect whose nature is quite different from the Pauli magnetism. They describe second-order processes where the staggered magnetization, whose wave vector is \mathbf{G} , gives rise to quantum transitions of electrons between states with the wave vectors \mathbf{k} and $\mathbf{k} + \mathbf{G}$. The DW, whose relatively smooth profile is characterized by the wave vector \mathbf{f} , such that $f \ll G$, adds \mathbf{f} to \mathbf{G} . Therefore, the second-order scattering amplitude of electrons from a DW in an antiferromagnet carries terms of the form $(E_{\mathbf{k}+\mathbf{G}-\mathbf{f}} - E_{\mathbf{k}})^{-1}$, which are represented by $G_{\mathbf{k}-\mathbf{f}+\mathbf{G}}^i$ in Eq.(17). In this expression \mathbf{k} is close to the Fermi surface. Therefore, $(E_{\mathbf{k}+\mathbf{G}-\mathbf{f}} - E_{\mathbf{k}})^{-1}$ becomes large if this surface is close to the nesting condition and \mathbf{G} coincides with the nesting vector. This leads to the enhancement of the effect of second-order terms Eqs.(14) and (15). Moreover, this expression becomes strongly dependent on \mathbf{f} , although the latter is much smaller than \mathbf{G} . On the other hand, when the Fermi surface is far from the nesting conditions this dependence is weak and the scattering amplitude may be expanded in powers of $\mathbf{v}_F \mathbf{f}$, where \mathbf{v}_F is the Fermi velocity. Since \mathbf{f} is associated with the coordinate gradients of the form $\mathbf{n}(\mathbf{r}, t) \times \nabla^i \mathbf{n}(\mathbf{r}, t)$ in the induced spin density. Such sort of terms, with $\mathbf{n}(\mathbf{r}, t)$ substituted for the ferromagnetic order parameter $\mathbf{m}(\mathbf{r}, t)$, were discussed in connection with the spin pumping from a ferromagnetic DW into a 3D metal film.²⁷

B. Disorder effects

In this subsection we shall consider effects of disorder on 2D electrons. Besides the usual potential scattering from impurities the spin-dependent scattering will also be taken into account. The latter leads to spin relaxation of electrons. A short-range impurity scattering potential will be assumed. In this case, the scattering amplitude from a single impurity has the form²⁸

$$f(\mathbf{k}, \mathbf{k}') = a + ib \boldsymbol{\sigma} \cdot (\mathbf{k} \times \mathbf{k}') \quad (18)$$

The first term in this expression is the isotropic spin-independent amplitude, while the second one represents the spin-orbit scattering. In a 2D system both incident and scattered wave vectors, \mathbf{k} and \mathbf{k}' , respectively, lie in the same xy plane. Therefore, only the σ_z Pauli matrix enters in the amplitude of the spin-orbit scattering. Therefore, the scattering probability, which is presumably given by the second-order Born approximation over the scattering amplitude, is spin-independent. As follows from Ref.[28], the total elastic scattering rate of electrons can be expressed as a sum of spin dependent and spin independent scattering channels. Accordingly, it can be written as²⁸

$$\Gamma = 1/2\tau = \pi N_F (a^2 + \frac{k_F^4}{2} b^2), \quad (19)$$

where τ is the elastic scattering time, while N_F and k_F are the state density and the Fermi wave-vector, respectively. At the same time, the retarded and advanced unperturbed Green's functions take the form²⁸

$$G_{\mathbf{k}}^r(\omega) = G_{\mathbf{k}}^a(\omega)^* = \frac{1}{\omega - E_{\mathbf{k}} - \mu + i\Gamma}, \quad (20)$$

where μ is the chemical potential.

Multiple scattering events should be taken into account in order to study the particle diffusion and spin relaxation effects. These effects are determined by the vertex function $\mathbf{V}(\omega, \mathbf{q})$ in Eqs.(12) and (14). With spin-independent Green functions Eq.(20) in hand the vertex \mathbf{V} can be easily calculated by summation of ladder diagrams. It is convenient to use its vector components V^l ($l = x, y, z$) which are given by $V^l \mathbf{e}^l = (1/2)\text{Tr}[\mathbf{V}\sigma^l]$ ($l = x, y, z$), where \mathbf{e}^l is the unit vector in the l -direction. In more detail the calculation of V^l is presented in Appendix A. Within the diffusion approximation, which is valid at $\omega \ll \Gamma$ and $qv_F \ll \Gamma$, the sum of the ladder diagrams is given by the diffusion propagator

$$V^l(\omega, \mathbf{q}) = \frac{2\Gamma}{i\omega - Dq^2 - \Gamma_s^l}, \quad (21)$$

where the spin relaxation rates Γ_s^l are $\Gamma_s^x = \Gamma_s^y = \pi N_F k_F^4 b^2$, $\Gamma_s^z = 0$ and the diffusion constant $D = v_F^2 \tau / 2$. It should be noted that the spin relaxation turns to zero when $l = z$ in Eq.(21). It occurs because the spin projection on the z -axis is conserved due to a specific form of the spin-orbit scattering amplitude, which is proportional to σ_z in a 2D gas. In this situation other mechanisms of the spin relaxation should be taken into account. However, such a strong spin relaxation channel as the scattering on AFM magnons can be efficient only at high enough temperatures. At low temperatures, due to the Fermi-liquid character of the electron gas, such an inelastic mechanism is weak, even in the absence of a gap in the excitation spectrum of magnons. The same can be said about the spin-lattice relaxation. The spin-orbit splitting of the conduction band might result in the spin relaxation through the D'yakonov-Perel mechanism²⁹. In

the considered here simple model, however, such sort of the spin-orbit coupling does not take place. Nevertheless, a weak Γ_s^z can be taken into account as a phenomenological parameter.

III. SPIN POLARIZATION OF ELECTRONS

A. Spin pumping by the staggered magnetization

Based on the general formalism presented in the previous section, let us consider the spin polarization which is produced in the normal metal by the exchange field of AFMI in the presence of a moving DW. As it was discussed in Sec.II there are two contributions to the spin polarization. Namely, the first-order effect due to the nonstaggered "ferromagnetic" magnetization and the second-order one produced by the staggered exchange field. The latter effect, which is given by Eqs.(14) and (15), will be considered in this subsection. Let us assume that within the classical theory the corresponding Néel vector $\mathbf{n}(\mathbf{r}, t)$ is given by the well known solution of the equation of motion for a one-dimensional DW in an uniaxial AFM.³⁰ The precession of $\mathbf{n}(\mathbf{r}, t)$ around the easy axis is assumed to be absent. It depends, however, on the method which is employed for the excitation of DW motion. For instance, the precession may be produced by the magnon's impact on the DW^{31,32}. Otherwise, the azimuthal angle of the Néel vector remains fixed during DW motion. The spin polarization of electrons, which can be induced by such DW, depends strongly on this angle. It becomes evident from the following consideration. Since \hat{G} in Eq.(10) is given by the unit matrix in the spin space (retarded and advanced functions are given by the spin-independent G^r and G^a in Eq.(20)), the spin structure of the function $\hat{\Sigma}$ in Eq.(10) is determined by the product $(\sigma_{\mathbf{n}_{\mathbf{f}^+, \nu^+}})(\sigma_{\mathbf{n}_{\mathbf{f}^-, \nu^-}}^*)$. Its spin-dependent part is given by $i\sigma(\mathbf{n}_{\mathbf{f}^+, \nu^+} \times \mathbf{n}_{\mathbf{f}^-, \nu^-}^*)$. Therefore, σ in this equation is perpendicular to the plane where the Néel vector of the DW resides. At the same time, this plane is fixed by the azimuthal angle of \mathbf{n} . In turn, as it follows from Eqs.(14),(16) and (21) the trace in Eq.(14) dictates that this spin direction must coincide with that of the vertex \mathbf{V} , whose vector components strongly depend on respective spin relaxation times. For example, if $\mathbf{n}(\mathbf{r}, t)$ belongs to the xy plane, the spin relaxation is given by Γ_s^z , which can be much smaller than Γ_s^x and Γ_s^y when the spin-orbit impurity scattering is a dominating mechanism of the spin relaxation. Below, let us assume that the easy axis of AFM is oriented parallel to the z -direction, while the DW moves in the x -direction with the velocity v . In this case the vector $(\mathbf{n}_{\mathbf{f}^+, \nu^+} \times \mathbf{n}_{\mathbf{f}^-, \nu^-}^*)$ lies in the xy -plane. Therefore, Γ_s^x and Γ_s^y enter in diffusion propagator Eq.(21). In the absence of precession around the easy axis the Néel vector is given in spherical coordinates by

$$\mathbf{n}(\mathbf{r}, t) = (\sin \theta \cos \phi, \sin \theta \sin \phi, \cos \theta), \quad (22)$$

where $\cos\theta = \tanh[(x - vt)/\lambda]$ and λ is the width of the DW, while ϕ is fixed. Below, for simplicity we choose $\phi = 0$. In this case the functions P^{ijk} in Eq.(16) are proportional to the Pauli matrix σ^y . As a result, by taking the trace in Eqs.(14) and (15) one obtains $\text{Tr}[\mathbf{V}\sigma^y] = 2V^y e^y$. Therefore, spins which are pumped into the 2D metal are oriented in the y -direction.

Parameters of the considered system are chosen in such a way that the wave vectors q and f in Eqs.(7)-(10) are much smaller than k_F . Similarly, the frequencies ω and ν are much smaller than the Fermi energy. For a steady moving DW the variables ω and q , as well as ν and f , are related to each other. Indeed, the Néel vectors $\mathbf{n}_{\mathbf{f}\pm, \nu\pm}$ in Eq.(10) can be written as

$$\mathbf{n}_{\mathbf{f}\pm, \nu\pm} = 2\pi\delta(\nu^\pm - v f_x^\pm) \int d\xi e^{-i f_x^\pm \xi} \mathbf{n}(\xi), \quad (23)$$

where $\xi = x - vt$. The delta-function in this relation fixes the frequencies $\nu^\pm = v f_x^\pm$. By combining $\nu^\pm = \nu \pm \omega/2$ and $f_x^\pm = f_x \pm q_x/2$ we find that $\nu = v f_x$ and $\omega = v q_x$. Note, that ω and q characterize the diffusion of electrons, because the diffusion propagator Eq.(21) depends on these variables. At the same time, ν and f are associated with variations of $\mathbf{n}(\mathbf{r}, t)$ within a DW. The integration over wavevectors and frequencies in Eq.(14) may be simplified at small ω and ν by replacing $\tanh(\Omega/k_B T)$ in Eq.(16) with $\tanh(\Omega/k_B T) - \tanh(\omega'/k_B T)$. Such a replacement does not change the result, because the terms in Eq.(14) that are proportional to $\tanh(\omega'/k_B T)$ cancel each other. Therefore, since $\Omega = \omega' \pm \omega/2$, or $\Omega = \omega' + \nu$, at the low temperature such a replacement restricts the integration over ω' to the range of small frequencies. As a result, the main contribution to the sum in Eq.(14) is given by vectors k which are close to the Fermi surface. Let us consider a simple tight binding model with the electronic band energy $E_{\mathbf{k}} = -\alpha(\cos k_x a + \cos k_y a)$. Note, that in this case $E_{\mathbf{k}} = -E_{\mathbf{k}+\mathbf{G}}$. Consequently, by integrating Eq.(14) over \mathbf{k} , in the leading approximation with respect to the small parameters $\omega/\Gamma, \nu/\Gamma, v_F q/\Gamma, v_F f/\Gamma$ and Γ/μ , we obtain the y -component $S_V^{y(2)}(\omega, \mathbf{q})$ of the vector $\mathbf{S}_V^{(2)}(\omega, \mathbf{q})$ in the form

$$S_V^{y(2)}(\omega, \mathbf{q}) = -i \frac{J^2 S^2}{\mu^2} V^y(\omega, \mathbf{q}) N_F(\mu) \times \int \frac{d\nu}{2\pi} \sum_{\mathbf{f}} \nu(\mathbf{n}_{\mathbf{f}+, \nu+} \times \mathbf{n}_{\mathbf{f}-, \nu-}^*), \quad (24)$$

where $N_F(\mu)$ is electronic state density at the chemical potential. Details of this calculation can be found in Appendix B. It is seen that $S_V^{y(2)}$ gives the main contribution in the spin density $\mathbf{S}^{(2)}$ which is a sum of $S_0^{y(2)}(\omega, \mathbf{q})$ and $S_V^{y(2)}(\omega, \mathbf{q})$. Indeed, it follows from a comparison of Eqs.(15) and (14) that these functions differ from each other by the absence in $S_0^{y(2)}(\omega, \mathbf{q})$ of the diffusion propagator $V^y(\omega, \mathbf{q})$. The latter, however, is much larger than one, because in the diffusion regime Γ is large in comparison with the denominator of Eq.(21). Therefore, $S_0^{y(2)}$ is

small compared with $S_V^{y(2)}$, so that the total spin density $\mathbf{S}^{(2)} = \mathbf{S}_0^{(2)} + \mathbf{S}_V^{(2)} \simeq \mathbf{S}_V^{(2)}$. It is important to note that $\mathbf{S}^{(2)}$ is proportional to μ^{-2} . Since the chemical potential is measured from the middle of the band, this dependence means that the pumping effect increases when μ approaches to the van Hove singularity. Such a dependence agrees with the discussed above role of the Fermi surface nesting in the spin pumping.

Note, that in the case of a 1D domain wall, which moves in the x -direction, the second line in Eq.(24) may be expressed as

$$\int \frac{d\nu}{2\pi} \sum_{\mathbf{f}} \nu(\mathbf{n}_{\mathbf{f}+, \nu+} \times \mathbf{n}_{\mathbf{f}-, \nu-}^*) = 2\pi i v \times \delta(\omega - v q_x) \delta_{q_y} \int d\xi e^{-i q_x \xi} (\mathbf{n}(\xi) \times \nabla_\xi \mathbf{n}(\xi)). \quad (25)$$

Therefore, by setting $\cos\theta = \tanh(\xi/\lambda)$ in Eq.(22) we obtain $(\mathbf{n}(\xi) \times \nabla_\xi \mathbf{n}(\xi)) = (1/\lambda) \cosh^{-1}(\xi/\lambda)$. Further, from Eqs.(21), (24) and (25) the spatial dependence of the induced spin density can be written as $S^{y(2)}(\mathbf{r}, t) = S^{y(2)}(\xi) = S_V^{y(2)}(\xi)$, where

$$S^{y(2)}(\xi) = \frac{J^2 S^2}{\mu^2} \int \frac{dq d\xi'}{2\pi\lambda} \frac{N_F v \Gamma}{\cosh \frac{\xi'}{\lambda}} \frac{\exp i q(\xi - \xi')}{D q^2 - i v q + \Gamma_s^y}. \quad (26)$$

By calculating the integral over q we arrive at

$$S^{y(2)}(\xi) = \frac{J^2 S^2}{2\mu^2} \frac{\Gamma N_F v}{\sqrt{v^2 + 4\Gamma_s^y D}} \int \frac{d\xi'}{\lambda} \frac{1}{\cosh \frac{\xi'}{\lambda}} \times \left(e^{-p_1 |\xi - \xi'|} \theta(\xi - \xi') + e^{p_2 |\xi - \xi'|} \theta(\xi' - \xi) \right), \quad (27)$$

where $p_1 = (1/2D)(v + \sqrt{v^2 + 4\Gamma_s^y D})$ and $p_2 = (1/2D)(v - \sqrt{v^2 + 4\Gamma_s^y D})$. These parameters determine widths of forward ($1/p_1$) and backward ($1/p_2$) diffuse propagations of the spin density with respect to the DW center. In most realistic cases these widths are much larger than the DW width λ . By taking into account that $D \sim v_F^2 \tau$ it follows from above expressions for p_1 and p_2 that $p_1 \lambda \ll 1$ and $p_2 \lambda \ll 1$, if $\max[v_F/v, 1/\sqrt{\Gamma_s \tau}] \gg \lambda/l$, where l is the electron's elastic mean free path. Typically $v_F/v \gg 1$ and $\Gamma_s \tau \ll 1$. Therefore, $p_1 \lambda$ and $p_2 \lambda$ are small, if the ratio λ/l is not too large. In this case the integration over ξ' in Eq.(27) is restricted to a small interval around $\xi' = 0$. Hence, by setting $\xi' = 0$ in Eq.(27) it may be simplified to

$$S^{y(2)}(\xi) = \frac{J^2 S^2}{2\mu^2} \frac{\pi \Gamma N_F v}{\sqrt{v^2 + 4\Gamma_s^y D}} \left(e^{-p_1 \xi} \theta(\xi) + e^{p_2 |\xi|} \theta(-\xi) \right). \quad (28)$$

Note, that the singularity of the derivative of $S^y(\xi)$ at $\xi = 0$ vanishes, when the actual profile of the DW in the integral over ξ' is taken into account. Such fine details, however, are not important, because the above expression is valid only in the range of distances from DW which are much larger than its width.

B. Spin polarization due to the nonstaggered magnetization of the domain wall

The polarization which is induced in the normal metal by the "ferromagnetic" part of the exchange field is given by Eqs.(12) and (13). For a one-dimensional DW moving with the velocity v in the x -direction $\mathbf{m}(\mathbf{r}, t) = \mathbf{m}(x-vt) \equiv \mathbf{m}(\xi)$. By performing Fourier transformation of $\mathbf{m}(\mathbf{r}, t)$ in Eq.(2) one can see that its Fourier transform $\mathbf{m}_{\mathbf{q}, \omega}$ is given by the right-hand side of Eq.(25) multiplied by the factor $-i/E_{\text{ex}}$. This expression should be substituted in Eq.(9) which, in turn, enters in Eqs.(12) and (13) for the spin density. By taking into account Eq.(21), in the leading approximation with respect to the small parameters ω/Γ and $v_F q_x/\Gamma$ the spin density $S^{(1)} = S_V^{(1)} + S_0^{(1)}$ can be written in the form

$$S^{y(1)}(\xi) = -i \frac{JS}{E_{\text{ex}}} N_F v \int \frac{dq d\xi'}{2\pi} \frac{\exp i q (\xi - \xi')}{\lambda \cosh \frac{\xi'}{\lambda}} \times \left[\frac{vq}{Dq^2 - ivq + \Gamma_s^y} - i \right]. \quad (29)$$

Similar to the previous subsection, at distances from DW which are larger than λ the integration over ξ' may be simplified, that results in

$$S^{y(1)}(\xi) = \frac{\pi JS N_F v}{E_{\text{ex}}} \times \left(\delta(\xi) + \frac{vp_1 e^{-p_1 \xi} \theta(\xi) + vp_2 e^{p_2 |\xi|} \theta(-\xi)}{\sqrt{v^2 + 4\Gamma_s^y D}} \right). \quad (30)$$

The first term in this expression is represented by the delta-function, as long as large distances are of interest, while in the range of DW it is given by the function $\pi^{-1} \lambda^{-1} \cosh^{-1}(\xi/\lambda)$, as it follows from the second term in the square brackets of Eq.(29).

IV. DISCUSSION

It was shown above that a moving DW in AFMI induces a macroscopic spin density in a 2D electron gas, which is in the epitaxial contact with the compensated surface of the AFMI. This spin density is a sum of two parts $\mathbf{S}^{(1)}$ and $\mathbf{S}^{(2)}$ whose y -components are given by Eqs.(27-28) and Eqs.(29-30). The spin polarization is perpendicular to the plane where the Néel vector of DW evolves. In the considered case it is the zx -plane, so that the polarization is parallel to the y -axis. The spin densities $\mathbf{S}^{(1)}$ and $\mathbf{S}^{(2)}$ have very different physical origins. Thus, $\mathbf{S}^{(1)}$ is induced by the nonstaggered part of the exchange field of a moving DW. It is determined by the Pauli magnetism in the first order with respect to the exchange interaction. At the same time, $\mathbf{S}^{(2)}$ is produced by the staggered Néel order in the second order with respect to J . It is instructive to compare these competing contributions to the total spin polarization

S. Let us consider the total polarization which is accumulated in the metal (per unit length of DW in the y -direction). By integrating spin densities Eq.(28) and Eq.(30) over x we obtain $S_{\text{tot}}^{y(1)} = \pi(JS/E_{\text{ex}})N_F v$ and $S_{\text{tot}}^{y(2)} = (J^2 S^2/\mu^2)(\Gamma/\Gamma_s^y)N_F v$. First, it should be noted a fundamental difference between these two spin densities. The effect of the staggered magnetization $S_{\text{tot}}^{(2)}$ diverges when the spin relaxation rate $\Gamma_s \rightarrow 0$,³³ while $S_{\text{tot}}^{(1)}$ does not depend on the spin relaxation. The reason is that the former effect is based on spin pumping from AFM into the metal. In the absence of spin relaxation such a pumping leads to steady increase of the spin polarization in the metal, until it saturates due to the spin relaxation. At the same time, the nonstaggered exchange field gives rise to the spin polarization through the Pauli mechanism. The motion of DW results only in redistribution of this polarization over the 2D metal. From a comparison of $S_{\text{tot}}^{y(1)}$ and $S_{\text{tot}}^{y(2)}$ it is seen that the pumping mechanism dominates at $JS > (\Gamma_s^y/\Gamma)(\mu^2/E_{\text{ex}})$. For instance, at $JS/\mu = 0.1$ and $\mu \sim E_{\text{ex}}$ the above inequality is fulfilled at $\Gamma_s^y/\Gamma \lesssim 0.1$, which always takes place if the spin relaxation is determined by the spin-orbit impurity scattering. This is because Γ_s is a relativistic correction to Γ , which is given by the nonrelativistic potential scattering. Also, μ must be close enough to zero, where the van Hove singularity just in the middle of the band is placed. In the above evaluation μ was assumed to be comparable with the exchange energy of spins in AFM, but much larger than the exchange interaction of itinerant and AFM interface spins. In turn, μ is much less than the Fermi energy that is counted from the bottom of the electronic energy band. As long as the effect of the staggered DW's magnetization dominates, let us further focus on a discussion of this effect.

As it follows from Eqs.(27) and (28), the pumped spin density is distributed asymmetrically with respect to DW. A tail of spin polarized electrons extends behind the moving DW over the distance $\sim p_2^{-1}$, which increases up to ∞ when $v \gg v_F \sqrt{\Gamma_s \tau}$. At the same time, ahead of DW the spin density extends up to $\sim p_1^{-1}$ which is always smaller than $l(\sqrt{(v^2/v_F^2) + \Gamma_s \tau})^{-1/2}$. The magnitude of the induced magnetization is largest at the center of the DW. From Eq.(28) one can evaluate it as

$$S^y(0) = N_F \Gamma \frac{J^2 S^2}{\mu^2} \frac{v}{\sqrt{v^2 + 4\Gamma_s^y D}}. \quad (31)$$

This expression turns to 0 at $v = 0$ and reaches its maximum when the DW velocity $v \gg \sqrt{\Gamma_s^y D} \sim v_F \sqrt{\Gamma_s \tau}$, by taking into account that $D = v_F^2 \tau/2$. Further, we notice that S^y increases as μ^{-2} at $\mu \rightarrow 0$ where the Fermi level approaches the middle of the band. This position of μ corresponds to the nesting condition for the Fermi surface, when $E_{\mathbf{k}_F} = E_{\mathbf{k}_F + \mathbf{G}}$. It agrees with the qualitative behavior of the second-order scattering of 2D electrons from an AFMI spin texture, which was discussed in SecIIA. On the other hand, one should take into account that in a 2D electronic system, which makes a con-

tact with AFM, the exchange interaction with localized spins results in the energy gap $2JS$ at $\mu = 0$.¹ Therefore, within the chosen tight binding model the chemical potential can not be placed too close to the middle of the band. Hence, it will be assumed that $|\mu| \gg JS$. In order to evaluate quantitatively the effect of spin pumping by a DW, it is convenient to compare it with the spin polarization which could be produced in the electron gas by an external static magnetic field H_{eff} . Since this spin polarization is $N_F \mu_B H_{\text{eff}}$, we get $\mu_B H_{\text{eff}} = S^y(0)/N_F$, where $S^y(0)$ is given by Eq.(31). From this equation one can see that in the case when $\Gamma_s^y D/v^2 \gg 1$ the effective magnetic field $\mu_B H_{\text{eff}} \sim \Gamma(J^2 S^2/\mu^2)(v/v_F)(\Gamma_s^y \tau)^{-1/2}$ (it was taken into account that $D = v_F^2 \tau/2$). By assuming $\tau = 10^{-13}\text{s}$, $\Gamma_s^y = 10^9\text{s}^{-1}$, $v_F = 10^5\text{m/s}$, $v = 100\text{m/s}$, $(J^2 S^2/\mu^2)=0.01$, and $\Gamma = (\hbar/2\tau) \sim 3\text{meV}$, we obtain $\mu_B H_{\text{eff}} = 0.003\text{meV}$, or $H_{\text{eff}} \sim 0.05\text{T}$. In this parameter range the induced spin polarization linearly increases with the velocity of DW. As shown in Refs.[31,32], in AFM insulators spin waves provide an efficient mechanism for DW propulsion. A more efficient effect may be realized due to the so called staggered torque effect, which is produced by electric current in a metallic AFM.²¹ Such a mechanism, however, cannot be implemented in AFM insulators. On the other hand, it might

be efficient in bilayers of 2D AFM insulators and metals. Regarding the magnon's effect, the relatively high value $v \sim 100\text{m/s}$ was calculated³¹ for circularly polarized magnons, while linearly polarized magnons produce much weaker effect. It should be noted that in the former case magnons cause precession of DW, so that the axial angle in Eq.(22) varies as $\phi = \Omega t$. As a result, the induced spin density will oscillate, in contrast to the stationary spin density soliton given by Eq.(28). Moreover, the spin polarization vector will have not only S^y components. Such a situation was not analyzed in this work. Also, a further analysis is necessary of the physics close to the nesting point, as it was discussed in the end of Sec.IIA.

The spin polarization, which is pumped by DW, can be detected by measuring the electric current in a heavy metal contact. The contact may be placed at the right edge of the junction which is shown in Fig.1. The current can be produced by the inverse spin Hall effect, or spin galvanic effect due to the strong spin-orbit coupling of electrons in the heavy metal. This method is usually applied for detection of the pumped spin polarization.¹ In the considered set up a DW arriving at the edge of AFM will inject the spin polarization into the contact and produce a pulse of the electric current there.

-
- ¹ V. Baltz, A. Manchon, M. Tsoi, T. Moriyama, T. Ono, Y. Tserkovnyak, *Rev. Mod. Phys.* **90**, 015005 (2018).
- ² O. Gomonay, V. Baltz, A. Brataas, Y. Tserkovnyak, *Nat. Phys.* **14** 213 (2018)
- ³ H. Yan, Z. Feng, P. Qin, X. Zhou, H. Guo, X. Wang, H. Chen, X. Zhang, H. Wu, C. Jiang, Z. Liu, *Adv. Materials* **32**, 1905603 (2020)
- ⁴ P. Wadley, B. Howells, J. Železný, C. Andrews, V. Hills, R. P. Campion, V. Novak, K. Olejnik, F. Maccherozzi, S. S. Dhesi, S. Y. Martin, T. Wagner, J. Wunderlich, F. Freimuth, Y. Mokrousov, J. Kunes, J. S. Chauhan, M. J. Grzybowski, A. W. Rushforth, K. W. Edmonds, B. L. Gallagher, T. Jungwirth, *Science*, **351**, 587 (2016).
- ⁵ J. Železný, H. Gao, K. Výborný, J. Zemen, J. Mašek, A. Manchon, J. Wunderlich, J. Sinova, and T. Jungwirth, *Phys. Rev. Lett.* **113**, 157201 (2014)
- ⁶ R. Cheng, J. Xiao, Q. Niu, and A. Brataas, *Phys. Rev. Lett.* **113**, 057601 (2014).
- ⁷ Saidaoui, H. B. M., A. Manchon, and X. Waintal, *Phys. Rev. B* **89** 174430 (2014).
- ⁸ A. C. Swaving and R. A. Duine, *Phys. Rev. B* **83**, 054428 (2011).
- ⁹ S. Takei, B. I. Halperin, A. Yacoby, and Y. Tserkovnyak, *Phys. Rev. B* **90**, 094408 (2014)
- ¹⁰ A. S. Núñez, R. A. Duine, P. M. Haney, and A. H. MacDonald, *Phys. Rev. B* **73**, 214426 (2006)
- ¹¹ Y. Ohnuma, H. Adachi, E. Saitoh, and S. Maekawa, 2014, *Phys. Rev. B* **89**, 174417.
- ¹² P. Zhang, C. T. Chou, H. Yun, B. C. McGoldrick, J. T. Hou, K. A. Mkhoyan, and L. Liu, arXiv:2201.04732
- ¹³ E. Cogulu, H. Zhang, N. N. Statuto, Y. Cheng, F. Yang, R. Cheng, and A. D. Kent, arXiv:2112.12238
- ¹⁴ K. A. Omari, L. X. Barton, O. Amin, R. P. Campion, A. W. Rushforth, P. Wadley and K. W. Edmonds, *Journal of Applied Physics* **127**, 193906 (2020)
- ¹⁵ L. Frangou, S. Oyarzun, S. Auffret, L. Vila, S. Gambarelli, and V. Baltz, *Phys. Rev. Lett.* **116**, 077203 (2016)
- ¹⁶ P. Vaidya, S. A. Morley, J. Tol, Y. Liu, R. Cheng, A. Brataas, D. Lederman and E. Barco, *Science*, **368**, 160 (2020)
- ¹⁷ J. Li et al. , *Nature* **578**, 70 (2020).
- ¹⁸ H. Wang, Y. Xiao, M. Guo, E. L. Wong, G. Q. Yan, R. Cheng, C. R. Du, *Phys. Rev. Lett.* **127**, 117202 (2021)
- ¹⁹ Y. Tserkovnyak, A. Brataas, and G. E. W. Bauer, *Phys. Rev. Lett.* **88**, 117601 (2002)
- ²⁰ R. Lebrun, A. Ross, S. A. Bender, A. Qaiumzadeh, L. Baldtrati, J. Cramer, A. Brataas, R. A. Duine, M. Kläui, *Nature* **561** 222 (2018)
- ²¹ O. Gomonay, T. Jungwirth, and J. Sinova, *Phys. Rev. Lett.* **117**, 017202 (2016)
- ²² S. K. Kim, G. S. D. Beach, K.-J. Lee, T. Ono, Th. Rasing, and H. Yang, *Nat. Mater.* **21**, 24 (2022).
- ²³ L. V. Keldysh, *Zh. Eksp. Teor. Fiz.* **47**, 1515 (1964) [*Sov. Phys. JETP* **20**, 1018 (1965)].
- ²⁴ V. G. Bar'yakhtar, B. A. Ivanov, M. V. Chetkin, *Sov. Phys. Usp.* **28**, 563 (1985) [*Usp. Fiz. Nauk*, **146**, 417 (1985)]
- ²⁵ J. Rammer, H. Smith, *Rev. Mod. Phys.* **58**, 323 (1986).
- ²⁶ B. L. Altshuler and A. G. Aronov, in *Electron-Electron Interactions in Disordered Systems*, edited by A. L. Efros and M. Pollak (North-Holland, Amsterdam, 1985).
- ²⁷ E. van der Bijl, R. E. Troncoso, and R. A. Duine, *Phys. Rev. B* **88**, 064417 (2013).
- ²⁸ A. A. Abrikosov, L. P. Gor'kov, *Sov. Phys. JETP* **15**, 752 (1962) [*Zh. Eksp. Teor. Fiz.* **42**, 1088 (1962)].

- ²⁹ M. I. D'yakonov and V. I. Perel', Sov. Phys. JETP **33**, 1053 (1971) [Zh. Eksp. Teor. Fiz. **60**, 1954 (1971)].
- ³⁰ N. L. Schryer and L. R. Walker, J. Appl. Phys. **45**, 5406 (1974).
- ³¹ E. G. Tveten, A. Qaiumzadeh, and A. Brataas, Phys. Rev. Lett. **112**, 147204 (2014)
- ³² S. K. Kim, Y. Tserkovnyak, and O. Tchernyshyov, Phys. Rev. B **90**, 104406 (2014)
- ³³ When the pumped polarization becomes too large the feedback effect should be taken into account. This situation needs an additional analysis.

Appendix A: Calculation of the vertex function $\mathbf{V}(\mathbf{q}, \omega)$

A single element of the ladder array, which corresponds to the Bethe-Salpeter equation in Fig. 2, is given by

$$\psi_0^{ij} = \frac{1}{2} \sum_{\mathbf{k}} \text{Tr}[\sigma^i G^r(\omega'^+, \mathbf{k}^+) f(\mathbf{k}^+, \mathbf{k}^+) \sigma^j \times f(\mathbf{k}^-, \mathbf{k}^-) G^a(\omega'^-, \mathbf{k}^-)], \quad (\text{A1})$$

where G^r and G^a are given by Eq.(20), Since $\omega' \ll \mu$ the integration in Eq.(A1) is restricted to $k \simeq k_F$. Therefore, one may set $|\mathbf{k}^\pm| = k_F$ and $|\mathbf{k}^{\pm'}| = k'_F$ in the scattering amplitude f , which is given by Eq.(18). Note, that in general, for a nonspherical Fermi surface $k_F \neq k'_F$. Further, as was noted in the main text, the spin-dependent part of f is proportional to σ_z . Hence, by calculating the trace in Eq.(A1) one may express it in the form

$$\frac{1}{2} \text{Tr}[\sigma^i f(\mathbf{k}^+, \mathbf{k}^+) \sigma^j f(\mathbf{k}^-, \mathbf{k}^-)] = a^2 \delta^{ij} + b^2 k_F^2 k_F'^2 (1 - (\hat{\mathbf{k}} \hat{\mathbf{k}}')^2) (\delta^{iz} \delta^{jz} - \delta^{ix} \delta^{jx} - \delta^{iy} \delta^{jy}), \quad (\text{A2})$$

where $\hat{\mathbf{k}}$ and $\hat{\mathbf{k}}'$ are unit vectors which are parallel to \mathbf{k} and \mathbf{k}' , respectively. Let us assume, for simplicity, that the Fermi line has an approximately circular form, which takes place if the chemical potential is sufficiently far from the middle of the considered tight binding band. In this case after integration in Eq.(A1) over $|\mathbf{k}|$ and by taking into account Eq.(A2) we obtain

$$\psi_0^{zz} = 2\pi i N_F \int \frac{d\phi}{2\pi} \frac{a^2 + b^2 k_F^4 (1 - (\hat{\mathbf{k}} \hat{\mathbf{k}}')^2)}{\omega - \mathbf{v}_F \mathbf{q} + 2i\Gamma} \quad (\text{A3})$$

and

$$\psi_0^{xx} = \psi_0^{yy} = 2\pi i N_F \int \frac{d\phi}{2\pi} \frac{a^2 - b^2 k_F^4 (1 - (\hat{\mathbf{k}} \hat{\mathbf{k}}')^2)}{\omega - \mathbf{v}_F \mathbf{q} + 2i\Gamma}, \quad (\text{A4})$$

where ϕ is the polar angle of the vector $|\hat{\mathbf{k}}|$. These functions depend on the angle between \mathbf{k}' and \mathbf{q} . This dependence originates from the second term in integrands of Eqs.(A3) and (A4), which, in turn, is proportional to the spin-orbit scattering amplitude b . The latter is much

weaker than the usual potential scattering a . Therefore, in the leading approximation the vertex function is angular independent. Hence, within this approximation Eqs.(A3) and (A4) can be averaged over directions of k' . By expanding them over ω , q and b up to their respective leading orders, after averaging over $\hat{\mathbf{k}}'$ and by substituting Γ from Eq.(19), we arrive at

$$\begin{aligned} \psi_0^{xx} = \psi_0^{yy} &= 1 + \frac{1}{2\Gamma} (i\omega - Dq^2 - 2\pi N_F b^2 k_F^4); \\ \psi_0^{zz} &= 1 + \frac{1}{2\Gamma} (i\omega - Dq^2). \end{aligned} \quad (\text{A5})$$

By summing the ladder diagrams the vertex function V^l can be expressed in terms of ψ_0 as

$$V^l = \frac{1}{1 - \psi_0^l}. \quad (\text{A6})$$

Finally, by substituting ψ_0^l from Eq.(A5) we obtain Eq.(21).

Appendix B: Calculation of the spin density

In this section the calculation is presented of the spin density, starting from Eq.(14). There are four terms, namely $P^{raa}(\omega'^+)$, $P^{rra}(\omega'^-)$, $P^{rra}(\omega' + \nu)$, and $P^{raa}(\omega' + \nu)$ in the right hand side of this equation. Each of these terms is proportional to the Fermi statistical factors in the form of $\tanh[(\omega' + \omega_i)/2k_B T] - \tanh[\omega'/2k_B T]$, where $\omega_i = \pm\omega$, or $\omega_i = \nu$. Since these frequencies are small, all these terms give small contribution to the spin density. However, the first two of them are much smaller than the third one. The reason is that the former are proportional to ω , while the latter $\sim \nu$. However, the function $\Sigma_{\mathbf{k}}^i(\omega', \omega; \nu, \mathbf{f})$ in Eq.(16) is an odd function with respect to change of signs of ν and \mathbf{f} , because two Néel vectors in Eq.(10) form a cross product, as it was explained in subsection III A. Indeed, $(\mathbf{n}_{\mathbf{f}^+, \nu^+} \times \mathbf{n}_{\mathbf{f}^-, \nu^-}^*)$ changes sign when $\nu \rightarrow -\nu$, $\mathbf{f} \rightarrow -\mathbf{f}$, because at such sign reversal $\mathbf{f}^\pm \rightarrow -\mathbf{f}^\mp$ and $\nu^\pm \rightarrow -\nu^\mp$. Hence, $\mathbf{n}_{\mathbf{f}^+, \nu^+} \leftrightarrow \mathbf{n}_{\mathbf{f}^-, \nu^-}^*$. Therefore, those terms which are proportional to ω have an additional small factor, because they must turn to zero with ν and f . In contrast, the term $\sim \nu$ is initially an odd function of ν . On this reason, it dominates in Eq.(14), as long as $\nu\Gamma \gg \omega \cdot \max(\nu, \nu_F f)$. By using Eq.(10) the contribution of this term in Eq.(14) can be written in the form

$$\begin{aligned} \mathbf{S}_V^{(2)}(\mathbf{q}, \omega) &= J^2 S^2 \frac{1}{2} \sum_{\mathbf{f}} \int \frac{d\nu}{2\pi} I(\omega, \mathbf{q}; \nu, \mathbf{f}) \times \\ &\text{Tr} \left[\mathbf{V}(\omega, \mathbf{q}) \left(\boldsymbol{\sigma} \cdot (\mathbf{n}_{\mathbf{f}^+, \nu^+} \times \mathbf{n}_{\mathbf{f}^-, \nu^-}^*) \right) \right], \end{aligned} \quad (\text{B1})$$

where

$$I(\omega, \mathbf{q}; \nu, \mathbf{f}) = \sum_{\mathbf{k}} \int \frac{d\omega'}{2\pi} G_{\mathbf{k}^+}^r(\omega'^+) G_{\mathbf{k}^-}^a(\omega'^-) (G_{\mathbf{k}+\mathbf{f}+\mathbf{G}}^r(\omega' + \nu) - G_{\mathbf{k}+\mathbf{f}+\mathbf{G}}^a(\omega' + \nu)) \left(\tanh \frac{\omega' + \nu}{k_B T} - \tanh \frac{\omega'}{k_B T} \right). \quad (\text{B2})$$

By substituting in this equation the expressions for Green functions from Eq.(5) and by expanding there the elec-

tron energy as $E_{\mathbf{k}+\mathbf{Q}} = E_{\mathbf{k}} + \mathbf{v}_{\mathbf{k}} \cdot \mathbf{Q}$, where $\mathbf{Q} = \mathbf{q}$, or \mathbf{f} and $\mathbf{v}_{\mathbf{Q}}$ is the velocity, the integral I can be written as

$$I(\omega, \mathbf{q}; \nu, \mathbf{f}) = \int \frac{d^2 k}{4\pi^2} \int \frac{d\omega'}{2\pi} \frac{1}{(\omega' + \frac{\omega}{2} - E_{\mathbf{k}} - \frac{\mathbf{v}_{\mathbf{k}} \mathbf{q}}{2} + \mu + i\Gamma)} \frac{1}{(\omega' - \frac{\omega}{2} - E_{\mathbf{k}} + \frac{\mathbf{v}_{\mathbf{k}} \mathbf{q}}{2} + \mu - i\Gamma)} \times \left(\frac{1}{(\omega' + \frac{\nu}{2} - E_{\mathbf{k}+\mathbf{G}} - \frac{\mathbf{v}_{\mathbf{k}+\mathbf{G}} \mathbf{f}}{2} + \mu + i\Gamma)} - \frac{1}{(\omega' + \frac{\nu}{2} - E_{\mathbf{k}+\mathbf{G}} - \frac{\mathbf{v}_{\mathbf{k}+\mathbf{G}} \mathbf{f}}{2} + \mu - i\Gamma)} \right) \left(\tanh \frac{\omega' + \nu}{k_B T} - \tanh \frac{\omega'}{k_B T} \right). \quad (\text{B3})$$

One should take into account that within the tight binding model $E_{\mathbf{k}+\mathbf{G}} = -E_{\mathbf{k}}$ and $v_{\mathbf{k}+\mathbf{G}} = -v_{\mathbf{k}}$. Then, it is seen that since $|\omega'| \sim |\nu| \ll \mu$, as well as ω , Γ , $v_{\mathbf{k}} q$ and $v_{\mathbf{k}+\mathbf{G}} f \ll \mu$ the major contribution to the integral at small T is given by two poles, whose wave vectors are close to the Fermi surface. Therefore, one can set $v_{\mathbf{k}} \simeq v_{\mathbf{k}_F} \equiv v_F$, where $E_{\mathbf{k}_F} = \mu$. In the leading approxi-

mation $\mu \gg \Gamma \gg [v_F q, v_F f, \nu, \omega]$ this integration gives

$$I(\omega, \mathbf{q}; \nu, \mathbf{f}) = -i \frac{\nu}{\mu^2} N_F. \quad (\text{B4})$$

By substituting this expression in Eq.(B1) we arrive at Eq.(24).